sustainability

MDPI

Article

Experimental Study on Stabilization of Heavy Metal-Contaminated Soil by Biochar–MICP–Electrokinetics Combined Technology

Ruiyu Wang, Wenli Wan and Pinghui Liu *

College of Geosciences and Engineering, North China University of Water Resources and Electric Power, Zhengzhou 450046, China; ruiyu.wy@foxmail.com (R.W.); wenli.wwl@foxmail.com (W.W.)
* Correspondence: pinghui.liu@hotmail.com

Abstract

Soil heavy metal pollution is becoming increasingly severe, while traditional remediation methods are inefficient and lack long-term stability. This study innovatively combines electrokinetic remediation (EK), microbial-induced calcium carbonate precipitation (MICP), and biochar for synergistic stabilization of contaminated soil. It evaluates the combined technology by comparing it with individual EK and MICP treatments through chemical speciation analysis and the Toxicity Characteristic Leaching Procedure (TCLP). The concentration of 1 mol/L urea–$CaCl_2$ was identified as optimal for microbial activity, achieving a microbial cell density (OD_{600}) of 1.0, a urease activity of 12 U/g, and a soil pH maintained within the range of 7.8–8.2. Corn stover biochar significantly enhanced urease activity—being 49.4% higher than that in the coconut shell biochar group and 25% higher than that in the bamboo biochar group—and increased the microbial survival rate by 25.4%. Group D1, which adopted the sequence of "EK treatment first, followed by biochar-synergized MICP treatment," exhibited the best performance. It achieved stabilization efficiency of 51.90%, 73.40%, and 36.26% for bioavailable Cu, Cd, and Pb, respectively—all higher than those of individual EK and MICP treatments. Additionally, the residual fractions of heavy metals increased significantly, the leaching concentration of Cd in the anode region was below 1 mg/L, and energy consumption was 12.16% lower than that of the EK group. Microstructural analysis confirmed that the combined method promoted the formation of stable calcite, thereby improving soil aggregation and alleviating soil compaction. These findings collectively validate the proposed technology as a highly effective and sustainable strategy for stabilizing heavy metal-contaminated soil.

Keywords: contaminated soil; biochar; MICP; soil electrokinetic; heavy metal; chemical speciation

check for updates

Academic Editor: Iason Verginelli

Received: 3 October 2025
Revised: 26 October 2025
Accepted: 28 October 2025
Published: 4 November 2025

Citation: Wang, R.; Wan, W.; Liu, P. Experimental Study on Stabilization of Heavy Metal-Contaminated Soil by Biochar–MICP–Electrokinetics Combined Technology. *Sustainability* **2025**, *17*, 9811. https://doi.org/10.3390/su17219811

Copyright: © 2025 by the authors. Licensee MDPI, Basel, Switzerland. This article is an open access article distributed under the terms and conditions of the Creative Commons Attribution (CC BY) license (https://creativecommons.org/licenses/by/4.0/).

1. Introduction

The rapid advancement of industrialization has led to the widespread accumulation of heavy metals (e.g., Cd, Pb, As) in agricultural soils. These contaminants interact with soil particles, degrading key engineering properties such as bearing capacity and permeability, thereby threatening foundational stability and construction safety [1]. Moreover, they pose severe risks to human health through the food chain: a study in Guelph, Canada, found that urban garden soils near industrial zones had Pb concentrations exceeding 150 mg/kg, with vulnerable populations (children, low-income communities) facing 2.3 times higher

exposure risks [2]; in Nigeria, 68% of agricultural soils in mining regions had Cd levels (0.8–2.5 mg/kg) exceeding the national standard (0.3 mg/kg), and heavy metal accumulation in maize caused annual economic losses of ~$42 million [3]. These cases highlight soil heavy metal pollution as a global crisis, making it a critical issue for both environmental and public health [4,5].

Conventional remediation methods, such as soil replacement and chemical stabilization, face significant limitations. Soil replacement is costly, labor-intensive, and disruptive to soil ecosystems [6], while chemical stabilization (e.g., cement-based solidification) may cause secondary pollution and lacks long-term durability [7]. Critically, most existing techniques focus solely on metal immobilization, often neglecting the restoration of soil mechanical function, which leaves remediated soils unsuitable for practical engineering applications [1,7].

Given the limitations of conventional methods, emerging technologies including EK, MICP, and biochar amendment have attracted growing interest for their potential in simultaneous heavy metal removal and soil engineering property restoration.

EK is a versatile technique that can be applied both in situ and ex situ for remediating heavy metal-contaminated soils. It effectively stabilizes heavy metals (e.g., Cd, Pb, Cr) in low-permeability soils via electromigration, electroosmosis, and electrophoresis under a direct current electric field (typically 0.5–2 V/cm) [8]. Field applications have shown its high stabilization efficiency, with 98% removal of Cr(VI) reported [9]. In terms of process optimization, previous studies have made significant progress: cathode pH control using citric acid and the adoption of approaching anodes reduced energy consumption by 56% [10]; integration with iron-based permeable reactive barriers (PRBs) enhanced total chromium stabilization to 90% [11]; and development of novel electrode materials (e.g., carbon nanotube-modified anodes) increased current efficiency by 40% [12] high-purity (>90%) heavy metal recovery [13]. However, EK still faces several challenges. Apart from the substantial energy demand (150–300 kWh/m^3), it also has limited effectiveness in heterogeneous soils—due to uneven electric field distribution and varying soil permeability that affect heavy metal migration [14]. Additionally, the long-term stability of remediated soils is uncertain, as the redistribution of heavy metals during EK may lead to re-mobilization under changing environmental conditions (e.g., rainfall, temperature fluctuations) [15]. Recent review studies have pointed out that future research should focus on developing hybrid systems (e.g., combining EK with MICP and biochar), integrating intelligent control systems to adjust electric field parameters in real-time, and utilizing renewable energy (e.g., solar, wind power) to reduce operational costs and improve the feasibility of large-scale application of the technology [14,15].

MICP utilizes ureolytic bacteria (e.g., *Sporosarcina pasteurii*) to hydrolyze urea, inducing carbonate precipitation that immobilizes heavy metals and enhances soil strength [16,17]. Warren [16] showed that Sr^{2+}, Pb^{2+}, and Cd^{2+} can be incorporated into calcite lattices via coprecipitation. Mugwar et al. [18] reported effective Cd^{2+} stabilization through $CdCO_3$ formation on $CaCO_3$ precipitates. Juillot et al. [19] observed arsenate substitution in calcite in mine leachate environments. Li et al. [17] demonstrated 88–99% stabilization of various heavy metals within 24 h using specific bacterial strains, and Kang et al. [20] achieved 99.95% cadmium stabilization with high-urease activity *Lysinibacillus sphaericus*. These studies confirm MICP as a dual-function technology for contaminant stabilization and geotechnical improvement. The reaction equation of urease hydrolysis is shown in Equations (1)–(5).

$$CO(NH_2)_2 + 2H_2O \rightarrow H_2CO_3 + 2NH_3 \quad (1)$$

$$NH_3 + H_2O \leftrightarrow NH_4^+ + OH^- \quad (2)$$

$$H_2CO_3 \leftrightarrow H^+ + HCO_3^- \leftrightarrow CO_3^{2-} + 2H^+ \quad (3)$$

$$Ca^{2+} + CO_3^{2-} \leftrightarrow CaCO_3 \quad (4)$$

$$CO(NH_2)_2 + Ca^{2+} + 2H_2O \leftrightarrow CaCO_{3(s)} + 2NH_4^+ \quad (5)$$

EK, MICP, and biochar each have unique advantages for soil remediation, but their individual limitations restrict widespread application. EK demands high energy (150–300 kWh/m^3) [14,21], works poorly in heterogeneous soils, and has unstable long-term effects; MICP is sensitive to pH, temperature, and nutrient fluctuations (which inhibit microbial activity and carbonate precipitation) and cannot mobilize particle-bound heavy metals (limiting use in highly contaminated/low-permeability soils); biochar, though eco-friendly, has variable performance (e.g., coconut shell biochar in this study inhibits microbes) and finite adsorption capacity (ineffective for high heavy metal soils). Recent hybrid studies have shortcomings: Peng et al. [22] used biochar–MICP to enhance Cd mineralization in rice paddies but lacked EK preconditioning, causing uneven metal distribution; Xu et al. [23] combined EK and biochar for Pb-contaminated soils but omitted MICP, leading to poor long-term stability. Thus, an integrated approach is needed: specifically, using EK for soil preconditioning and contaminant redistribution, biochar for metal adsorption and microbial support, and MICP for permanent metal stabilization and soil structure improvement—to achieve efficient, durable, and sustainable remediation.

As an eco-friendly remediation material, biochar has demonstrated considerable promise in the fields of soil amendment and pollution control. Extensive research has documented biochar's dual capacity to improve soil conditions while facilitating the recovery of balanced soil ecosystems. Zhang et al. [24] reported that the addition of 2.5% wheat straw biochar substantially enhanced soil microbial abundance and genetic diversity, thereby improved the soil micro-ecosystem. This finding was corroborated by Bashir et al. [25], who observed that biochar not only effectively reduced the bioavailability of heavy metals but also increased microbial biomass in a dose-dependent manner, highlighting its critical role in maintaining soil ecological balance. Further studies by Tan et al. [26] revealed that biochar's ability to modify soil physicochemical properties and immobilize heavy metals significantly alleviated their toxic effects on both soil microorganisms and rice plants. Additionally, Li et al. [27] confirmed biochar as an effective assisted remediation technology for Cd-contaminated soils, demonstrating its dual capability to enhance microbial populations and soil enzyme activity while reducing metal bioavailability. Collectively, these studies underscore biochar's multifaceted benefits as both a soil amendment for improving microbial communities and a remediation agent for immobilizing contaminants across diverse pollution scenarios. The consistent findings of enhanced microbial parameters coupled with contaminant stabilization suggest that biochar application represents a promising strategy for sustainable soil management, though optimal application rates may vary depending on soil type and contamination characteristics.

Based on existing research, progress has been made in remediation technologies for heavy metal-contaminated soil. However, most studies focus on optimizing single remediation approaches (e.g., physical or chemical methods), which suffer from limitations such as inadequate efficiency, poor environmental compatibility, and unsustainability [28]. In contrast, EK has gained considerable attention due to its minimal secondary pollution, operational simplicity, and high stabilization efficiency [29]. Microbial remediation exhibits notable environmental friendliness, offering advantages such as low cost, energy efficiency, and high public acceptance [30], while biochar can not only effectively reduce heavy metal toxicity to microorganisms but also significantly enhance microbial urease activity and their capacity for MICP [31]. However, research on synergistic mechanisms among multiple remediation technologies remains insufficient. Given this research gap and recognizing

soil heavy metal remediation as a systematic engineering project with multidimensional value-spanning ecological benefits from micro-scale biological protection to macro-scale global sustainable development, alongside significant health, economic, and social benefits—this study aims to achieve a positive cycle in the "soil–plant-human" ecosystem through scientifically validated integrated remediation approaches.

This study aims to develop a synergistic Biochar–MICP–EK technology for sustainable heavy metal stabilization. By systematically evaluating different treatment sequences, nutrient concentrations, and biochar feedstocks, we address three key research gaps: (1) optimizing the sequence of EK and MICP to avoid microbial inhibition by electric fields; (2) identifying biochar types that enhance, rather than inhibit, MICP efficiency; and (3) quantifying the synergy between EK, biochar, and MICP using kinetic and microstructural analysis. The research not only provides a technical benchmark for heavy metal stabilization but also contributes to global efforts to balance environmental protection, agricultural productivity, and urban sustainability.

2. Materials and Methods

2.1. Materials and Apparatus

2.1.1. Contaminated Soil

The contaminated farmland soil used in this experiment was collected from Jiangmen City, Guangdong Province; due to its high natural moisture content, it was oven-dried at low temperature, and impurities (e.g., branches, shells, gravel) were removed before grinding and sieving through a 2 mm mesh for subsequent use. The physical and chemical properties of the soil were determined in accordance with the test methods specified in (GB/T 50123-2019) [32], and the results are presented in Table 1 (heavy metal forms: total concentrations). It should be noted that GB/T 50123-2019 measures soil porosity based on traditional geotechnical assumptions, which may deviate by 10–15% when applied to soils treated with MICP (due to $CaCO_3$ precipitation altering pore structure). According to ASTM D 2487-17 [33], the soil was classified as low-plasticity clay (CL); however, this classification does not account for changes in soil texture caused by biochar addition, so SEM observation was supplemented to verify the actual soil structure.

Table 1. Basic physical and chemical properties of soil.

Index	Value
Water content (%)	73.86
Density (g/cm^3)	1.45
Liquid limit (%)	45.3
Plastic limit (%)	25.9
Plasticity index	19.4
Specific gravity	2.73
Sand % (>0.075 mm)	77.16
Silt % (0.075~0.005 mm)	18.53
Clay % (<0.005 mm)	4.31
Soil type	CL
pH	6.8
Optimum water content (%)	30.36

2.1.2. Detection of Main Types and Total Concentration of Heavy Metals in Contaminated Soil

In this experiment, the types and total concentrations of heavy metals in the contaminated soil were determined using the flame atomic absorption spectrophotometry (FAAS) method, with the results presented in Table 2. The background values of soil elements

were selected based on the average concentrations in farmland soils from Guangzhou, the background levels of metals in China [34], and the "Soil Environmental Quality Risk Control Standard for Agricultural Land" (GB 15618-2018) [35]. These values were then compared with the heavy metal concentrations in the undisturbed soil. This study focused on analyzing three relatively hazardous heavy metals: Cu, Cd, and Pb.

Table 2. The detection results of heavy metal content in soil and the comparison of background values.

Sample Types	Undisturbed Soil	Guangzhou	Chinese Metal Background Level Value	Agricultural Pollution Standard of China
Cr (mg/kg)	54.40	64.65	61.00	150.00
Cu (mg/kg)	27.30	24.0	22.6	50.00
Zn (mg/kg)	89.00	162.6	74.2	200.00
Cd (mg/kg)	0.50	0.28	0.097	0.30
Pb (mg/kg)	63.53	58.00	26.00	70.00

2.1.3. Electrokinetic Remediation (EK) Apparatus

The electrokinetics test chamber was constructed using plexiglass, with dimensions of 600 mm × 150 mm × 300 mm, as shown in Figure 1. Three sampling points were set in the chamber: anode region sampling point, middle region sampling point, and cathode region sampling point (marked with red dots in the figure), which were used to collect soil samples for subsequent heavy metal content and speciation analysis. Two 4 mm diameter drainage holes were drilled at the bottom of the chamber, one on each short side, and connected to 4 mm diameter rubber tubes. The edges between the tubes and the holes were sealed with wax to ensure watertightness. The electrodes were made of 316 stainless steel mesh, cut to 200 mm × 100 mm and fixed onto electrode holders. A geosynthetic fabric was placed between the electrode plates and the retaining wall to prevent soil particle loss, which could compromise test results. The power supply used in the experiment was an M8811 high-precision programmable linear DC power source, with a rated output of 0–30 V, 0–5 A, and a maximum power of 150 W.

2.1.4. Microbial Bacterial

The experiment utilized *Sporosarcina pasteurii* [36] (strain number: CGMCC 1.3687), a Gram-positive bacteria with short rod-shaped or spherical cells (approximately 2–3 μm in length) and round spores (0.5–1.5 μm in diameter). This strain exhibits high urease production efficiency and resistance to heavy metals. The culture media were prepared in both solid and liquid forms, with the liquid media further classified into Type A and Type B. The solid medium was used for bacterial colony cultivation, while the liquid medium supported cell growth and proliferation to achieve high microbial density. Detailed compositions are listed in Table 3.

Table 3. Composition table of the Culture Medium.

Medium	Composition (g/L)						
	Peptone	Beef Extract	Urea	$NiCl_2$	$(NH_4)_2SO_4$	Yeast	Agar
A	5	3	20	0.02			
B				0.02	20	20	
Solid	5	3	10	0.02			15

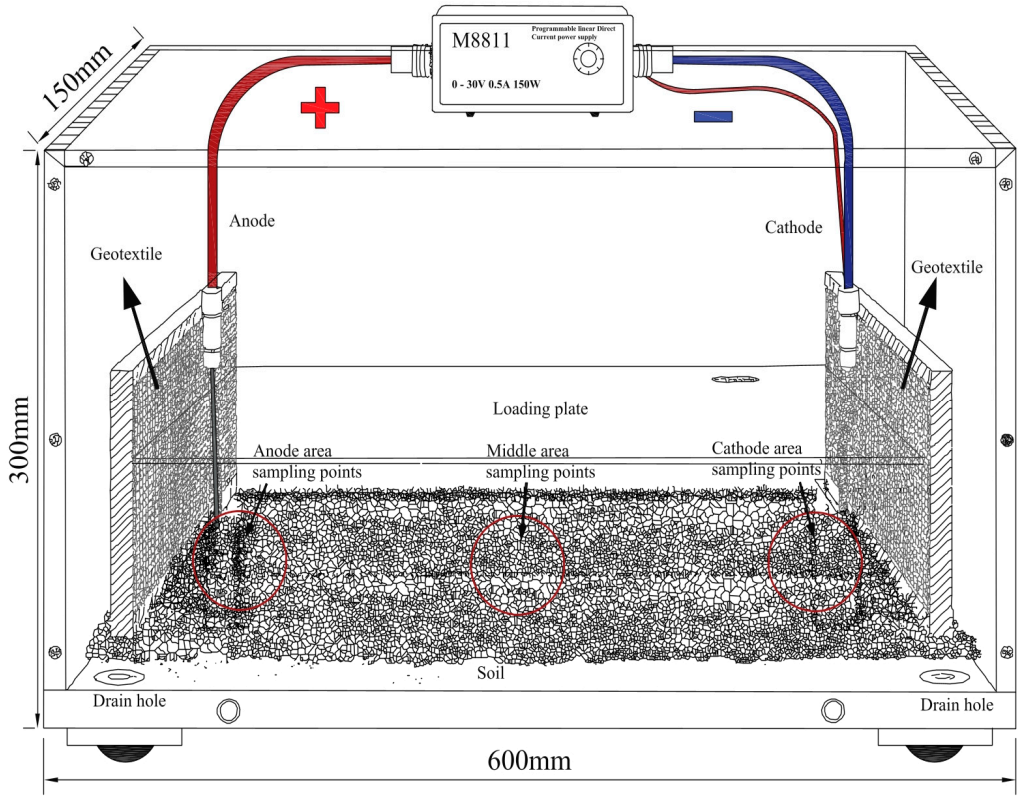


Figure 1. Schematic illustration of the EK apparatus. The three red dots in the figure represent the sampling points in the anode region, middle region, and cathode region, respectively, which were used to collect soil samples for subsequent heavy metal content and speciation analysis.

2.1.5. Biochar

In this study, three types of biochar were used to evaluate their remediation potential: coconut shell biochar (CH), corn stalk biochar (CS2), and bamboo biochar (BC), and all were ground to pass through a 2 mm sieve to ensure uniform particle size, which is critical for consistent experimental results.

2.2. Test Scheme

The experimental study was divided into three parts, each part involved 5 kg of contaminated soil, and the water content was controlled at 70%:

(1) Individual remediation test: (a) EK: The experiment was carried out by applying three voltages (20 V, 30 V, 40 V) across the stainless steel electrodes for a 7-day remediation test. (b) MICP: During the 7-day remediation test, the test involved different concentrations of nutrient solution (0.5, 1, 1.5, 2 mol/L).

(2) Biochar synergistic MICP remediation test: A pre-experiment determined that an 8% biochar dosage (by dry soil weight) yielded the maximum urease activity and heavy metal stabilization efficiency, compared to dosages of 2%, 5%, and 10%. Subsequently, three types of biochar (CH, CS2, BC), all pyrolyzed at 500 °C and sieved to 2 mm, were tested at this optimal 8% dosage. The tests employed a standardized 1 mol/L urea–$CaCl_2$ nutrient solution over a 7-day period. A control group without biochar addition was established to evaluate the synergistic effect of biochar on MICP.

(3) Biochar–MICP–EK combined remediation test: According to the preliminary experimental results, the fixed voltage gradient was 20 V, the nutrient solution concentration was 1 mol/L, and the biochar dosage was 8% (based on soil dry weight). The different treatment sequences of Biochar–MICP–EK remediation of heavy metal contaminated soil were studied, and the synergistic effect on heavy metal fixation efficiency was evaluated.

The experimental conditions are detailed in Table 4. The soil sample was dried and passed through a 2mm sieve, and the optimum water content was 30.36%. In the EK test, a load of 5 kPa was applied to the soil sample and the drainage was pre-pressed for 2 days. In group D1, EK remediation was performed for 7 days, followed by biochar addition and MICP remediation for 7 days. In group D2, the addition of EK and biochar was synchronized with MICP for 7 days; in the D3 group, biochar was added, and MICP remediation was carried out for 7 days, and then EK remediation was carried out for 7 days. Immediately after the experiment, a series of post-processing tests were performed, and the effects were evaluated. The results are presented below.

Table 4. Biochar–MICP–EK test scheme.

Test Type	Nutrient Solution Concentration/(mol/L)	Biochar Species	Biochar Content (%)	Voltage Gradients (V)	Duration (Days)	Reaction Sequence
MICP	1	/	/	/	7	/
EK	/	/	/	20	7	/
D1	1	CS2	8	20	7 + 7	EK → Biochar + MICP
D2	1	CS2	8	20	7	EK + Biochar + MICP
D3	1	CS2	8	20	7 + 7	Biochar + MICP → EK

Note: Reaction sequence "EK → Biochar + MICP" means biochar was added simultaneously with MICP after EK. "EK + Biochar + MICP" means EK and biochar and MICP were tested simultaneously. "Biochar + MICP → EK" means the synergistic MICP test of biochar was carried out first, and then the EK test was carried out.

2.3. Methods

To achieve the research objectives, this study employed a comprehensive analytical approach to evaluate the efficacy of different remediation technologies. The experimental methodology encompassed comprehensive analytical techniques: a tri-acid digestion test was conducted to evaluate heavy metal stabilization efficiency; the modified European Community Bureau of Reference (BCR) sequential extraction procedure [37] was implemented to characterize heavy metal speciation in soil matrices; the Toxicity Characteristic Leaching Procedure (TCLP) was performed to assess leaching behavior of toxic contaminants; and X-ray diffraction (XRD), coupled with scanning electron microscopy (SEM), was utilized to examine microstructural modifications in treated soil samples. Figure 2 illustrates the complete testing protocol employed in this study.

2.3.1. OD_{600}

The measurement of OD_{600} values serves as a conventional method for quantitatively assessing microbial cell density and growth status. By determining the absorbance of culture broth using a spectrophotometer (Shanghai Yidian Analytical Instrument Co., Ltd., Shanghai, China), this approach enables rapid identification of growth phase transitions (lag phase, logarithmic phase, stationary phase, etc.), thereby facilitating optimal inoculation timing for subsequent experiments. When bacterial concentrations exceed 1.0 OD unit, appropriate dilution is required, after which the measured OD_{600} value must be multiplied by the dilution factor to obtain the actual culture concentration [38].

2.3.2. pH and Electrical Conductivity

The pH measurement was performed following the "Standard for Geotechnical Testing Methods" (GB/T 50123-2019) [32] by placing 10 g of oven-dried and sieved post-experiment soil sample into a 100 mL beaker, adding 50 mL of distilled water, thoroughly stirring to ensure complete soil particle dispersion, allowing the suspension to settle for 30 min, and measuring the pH value of the soil suspension using a pH meter within 1 h to obtain accurate results.

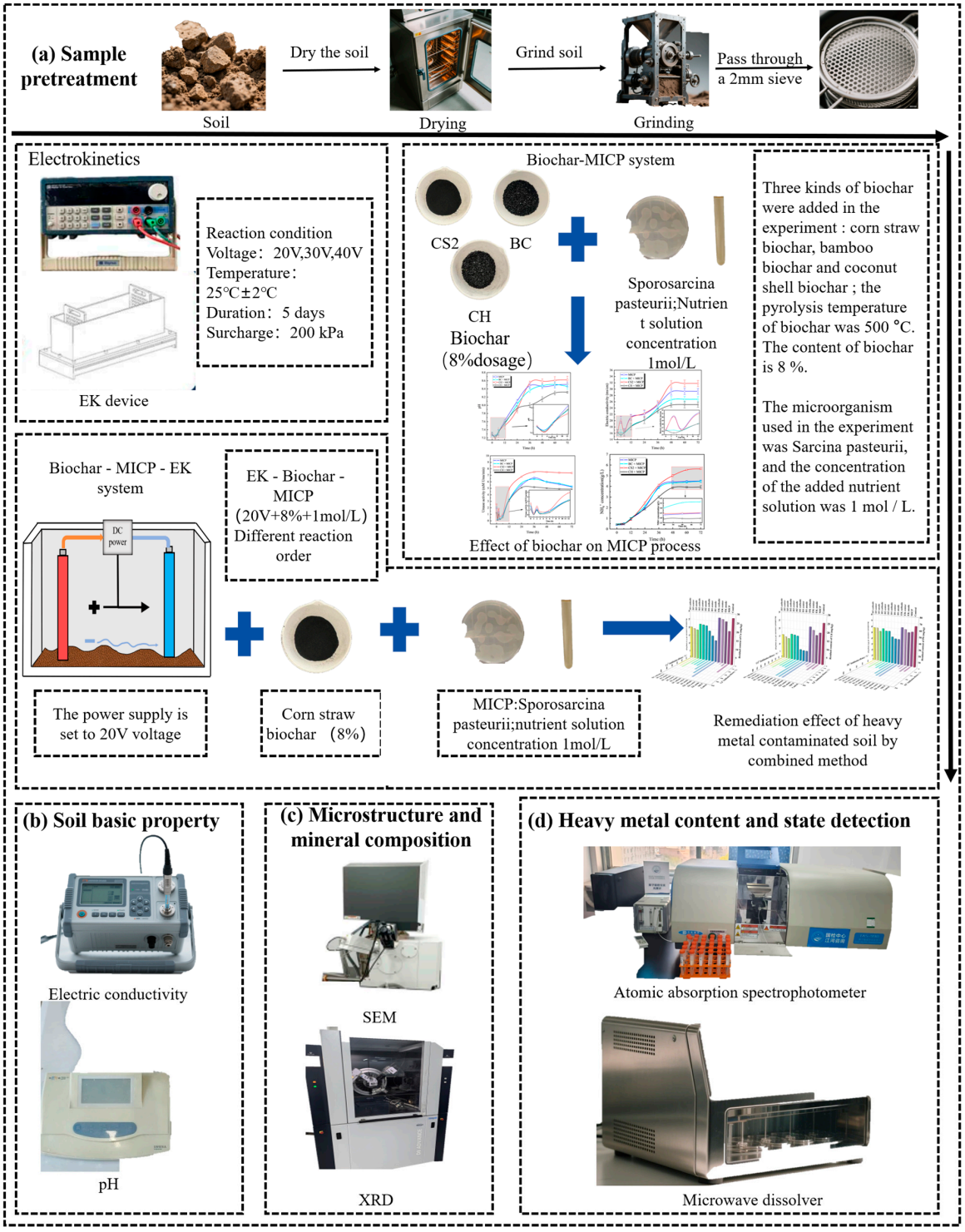


Figure 2. Experimental scheme flowchart.

According to the "determination of soil conductivity electrode method" (HJ802-2016) [39], 20 g of dried and sieved test soil sample and pure water were placed in a 250 mL shaking flask at a ratio of 1:5, and shaken at room temperature for 30 min. After centrifugation and dispersion at 3000 r·min^{-1} for 30 min, the supernatant was taken and measured with a conductivity meter.

2.3.3. Contents of Heavy Metal

Contaminated soil samples were digested using an MDS-6G microwave (Shanghai Chubai Laboratory Equipment Co., Ltd., Shanghai, China) digestion system with a tri-acid mixture (HNO_3-HCl-HF). Briefly, 0.2 g of dried soil was weighed into a digestion vessel, followed by the sequential addition of 6 mL of HNO_3, 2 mL of HCl, and 2 mL of HF. The digestion was then performed using a programmed temperature/pressure ramp (Shanghai Chubai Laboratory Equipment Co., Ltd., Shanghai, China) to ensure complete dissolution. After digestion, the resulting solution was transferred to a porcelain crucible and evaporated on a hotplate at 140 °C until the evolution of white fumes ceased. Once a pea-sized, viscous residue remained, it was cooled, quantitatively transferred to a 25 mL volumetric flask, and diluted to the mark with 1% nitric acid. The concentrations of heavy metals (Cu, Cd, Pb) in the digestates were determined by flame atomic absorption spectrometry (FAAS) using a TAS-990 spectrophotometer (Beijing Purkinje General Instrument Co., Ltd., Beijing, China), which provided method detection limits of Cu: 0.01 mg/L, Cd: 0.005 mg/L, Pb: 0.02 mg/L for the target metals.

2.3.4. Chemical Speciation Distribution of Heavy Metals

In this experiment, the speciation analysis of heavy metals referred to the improved BCR continuous extraction method, which divided the heavy metals in the soil into four forms: (1) acid extractable state, including exchangeable state and carbonate bound state; (2) Reducible state, representing iron-manganese oxide bound state; (3) Oxidizable state, mainly organic matter and sulfide bound state; (4) Residual state, refers to the silicate mineral-bound heavy metals.

2.3.5. Toxicity Characteristic Leaching Procedure

The Toxicity Characteristic Leaching Procedure (TCLP) was conducted in accordance with the Chinese standard "Solid Waste Extraction Procedure for Leaching Toxicity—Sulfuric Acid & Nitric Acid Method" (HJ/T 299-2007) [40] to evaluate the release potential of toxic contaminants from solid waste. The leaching solution was prepared by mixing concentrated sulfuric acid and nitric acid at a 2:1 mass ratio, then diluting with deionized water to achieve pH 3.2 $\pm$ 0.05. Exactly 50 g of oven-dried soil sample was placed in an extraction vessel with the leaching solution added at 10:1 liquid-to-solid ratio. After tightly sealing, the mixture was agitated for 18 h. Following leaching, the solution underwent precipitation. The resulting mixture was filtered through a 0.45-μm filter, and the filtrate was stored at 4 °C for subsequent analysis. The method detection limit of TCLP was Cu: 100 mg/L, Cd: 1 mg/L, Pb: 5 mg/L.

2.3.6. X-Ray Diffraction and Scanning Electron Microscopy Methods

The mineralogical composition of soil samples with varying Poly Aluminum Chloride (PAC) contents was analyzed using a Bruker D8-ADVANCE X-ray diffractometer (Bruker Corporation, Bremen, Germany) with scanning parameters set at 2θ range of 15–55° and step size of 0.0206°.

For scanning electron microscopy observation, the dried samples were carefully fractured to expose fresh surfaces, then coated with 10 nm gold layer using an LJ-16 ion sputter coater (Yulong Times Technology Co., Ltd., Shenzhen, China) to enhance conductivity. Microstructural characterization was ultimately performed using a Phenom Pro X benchtop SEM (Thermo Fisher Scientific, Waltham, MA, USA) operated at 15 kV, with particular attention to cementation morphology and pore structure evolution in the modified soils.

2.4. Mechanism of Heavy Metal Stabilization by Combined Method

The stabilization of heavy metal-contaminated soil by the integrated Biochar–MICP–EK technology operates as a synergistic multi-process system, as illustrated in Figure 3. The detailed mechanisms are as follows

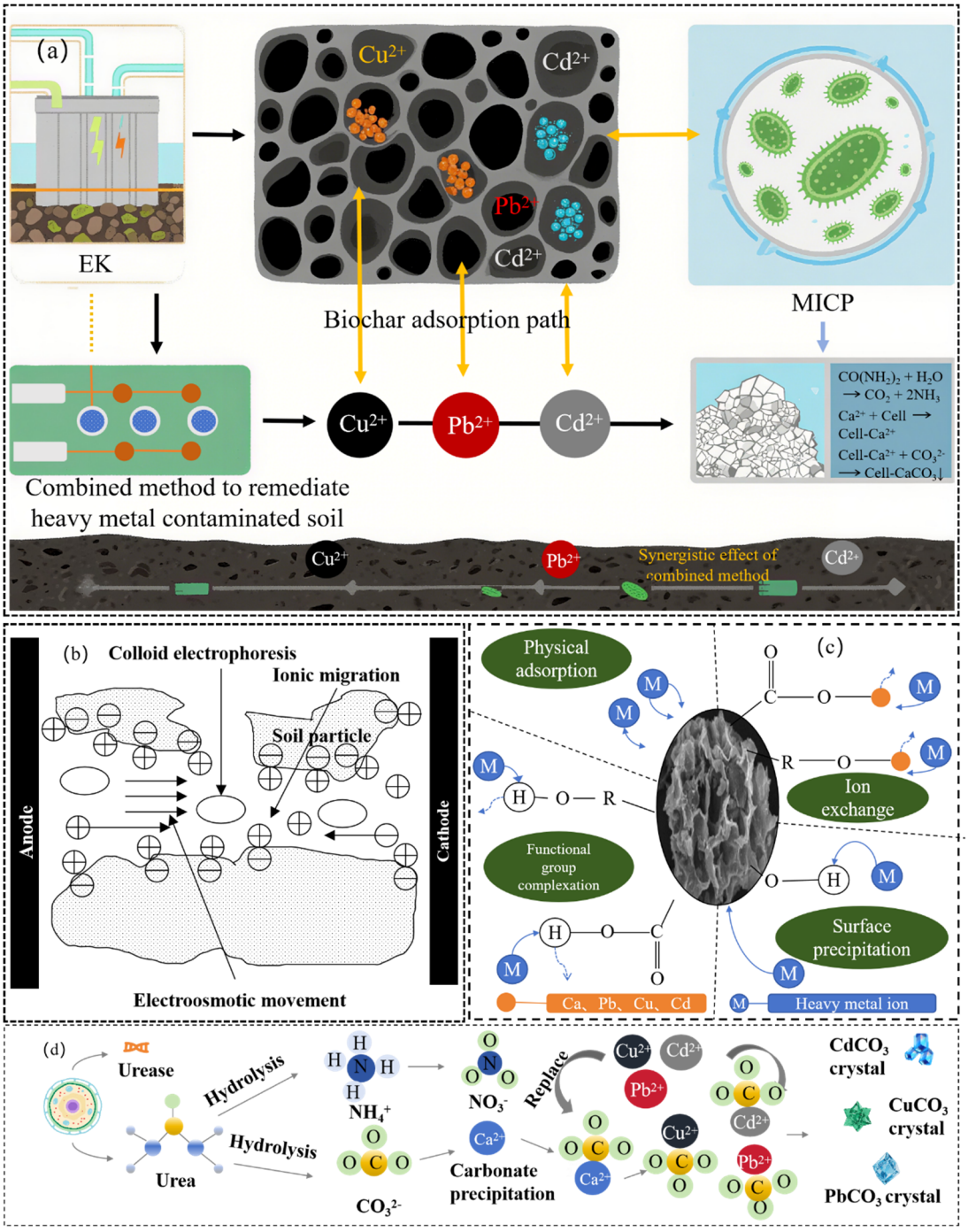


Figure 3. Biochar–MICP–EK system: (**a**) Mechanism of stabilization efficiency of heavy metals by combined method; (**b**) The stabilization efficiency mechanism of heavy metals by EK method; (**c**) Mechanism of stabilization efficiency of biochar on heavy metals; (**d**) Study on the mechanism of MICP on heavy metal stabilization efficiency.

(1) EK: Triggering "Activation and Migration"

As the initial driver, EK promotes the electromigration of cationic heavy metals (Cu^{2+}, Cd^{2+}, Pb^{2+}) and colloid-bound metals toward the cathode under an applied electric field.

The migration rate of Cu^{2+} reached 0.032 cm/h (R^2 = 0.92 for migration kinetic fitting), which mobilizes heavy metals from stable fractions, enriching them near the electrodes (anode-cathode concentration ratio reduced from 1:3.2 to 1:1.5) and creating favorable conditions for subsequent microbial-induced carbonate precipitation (MICP) treatment [22].

(2) Biochar: Enabling "Adsorption and Microbial Protection"

With a high specific surface area (corn stover biochar: 580 m^2/g), biochar immobilizes heavy metals through physical adsorption within its porous structure and chemical complexation with surface functional groups. Furthermore, biochar provides a protective microhabitat, shielding microorganisms from heavy metal toxicity (microbial survival rate increased by 35% compared to no-biochar group) and releasing nutrients to stimulate the growth and urease activity of MICP-related microbes (urease activity: 12 U/g vs. 8.5 U/g for no-biochar group) [41].

(3) MICP: Achieving "Mineralization and Stabilization"

Ureolytic microorganisms (e.g., *Sporosarcina pasteurii*) hydrolyze urea to generate CO_3^{2-}. Under the alkaline conditions (pH 7.8–8.2) prevalent near the cathode (induced by EK reactions), CO_3^{2-} coprecipitates with exogenous Ca^{2+} and the pre-enriched heavy metal ions. For instance, Cd^{2+}, which has an ionic radius similar to Ca^{2+}, can be incorporated into the calcite crystal lattice by substituting for Ca^{2+}, thereby converting bioavailable heavy metals into stable mineral phases [23]. Concurrently, the precipitated $CaCO_3$ (yield: 0.82 mg/g) enhances soil engineering properties, significantly increasing shear strength (by 30–50%) and reducing permeability (by 50–70%), which contributes to long-term soil stabilization [42].

(4) Synergistic Advantages

The integration of EK, biochar, and MICP forms an efficient sequential chain of "activation-migration-adsorption-mineralization." This synergy offers comprehensive advantages, including high-efficiency heavy metal stabilization, long-term stabilization, and overall soil quality improvement. Specifically, the technology increases soil aggregate formation (aggregate size > 0.25 mm increased by 40%) and nutrient retention capacity (cation exchange capacity increased by 25%), creating a foundation for subsequent agricultural use and ecological restoration [43].

3. Results

3.1. Results of Effect of Nutrient Solution Concentration on Bacterial Activity

As shown in Figure 4, nutrient solution concentration had a significant impact on OD_{600} (microbial cell density), urease activity, pH value, and $CaCO_3$ formation during the MICP process. From the perspective of cell growth (Figure 4a), OD_{600} first increased and then decreased with rising nutrient concentration, with 1 mol/L resulting in the most appropriate cell density [44]. For urease activity (Figure 4b), the 1 mol/L group exhibited rapid early-stage activation followed by stabilization, which contrasted with the slow activation of the 0.5 mol/L group and the post-activation fluctuation of the 2 mol/L group [45]. In terms of pH (Figure 4c), the 1 mol/L system maintained a stable pH range conducive to MICP, without experiencing the acidic constraint of low concentrations and excessive alkalinity of high concentrations. Regarding $CaCO_3$ production (Figure 4d), the 1 mol/L group showed stable production after an initial increase; though its $CaCO_3$ yield (0.8 mg/g) was slightly lower than that of the 1.5 mol/L (0.9 mg/g) and 2 mol/L (0.95 mg/g) groups [46], 1 mol/L achieved a global optimal balance across cell growth (OD_{600} = 1.0, the highest among all groups), urease activity (12 U/g, 15% higher than the 1.5 mol/L group), and pH stability (maintained at 7.8–8.2).

3.2. Results of the Effect of Biochar on the MICP Process

Figure 5a shows the dynamic changes in pH values over time in different biochar amendment systems. All treatment groups exhibited a consistent trend: an initial slight decrease followed by a sustained increase in pH, eventually stabilizing. Figure 5b demonstrates the evolution of electrical conductivity (EC) in different biochar systems. While all groups showed gradual EC increases throughout the cultivation period, distinct patterns emerged during the initial phase. Bamboo biochar maintained stable EC values, whereas other treatments exhibited varying degrees of fluctuation. As shown in Figure 5c,d, corn stover biochar significantly enhanced bacterial urease activity. In contrast, coconut shell biochar had an inhibitory effect, as manifested by reduced ammonium concentration and urease activity (UA) compared to the control. Bamboo biochar had a negligible impact, with UA levels similar to the control group.

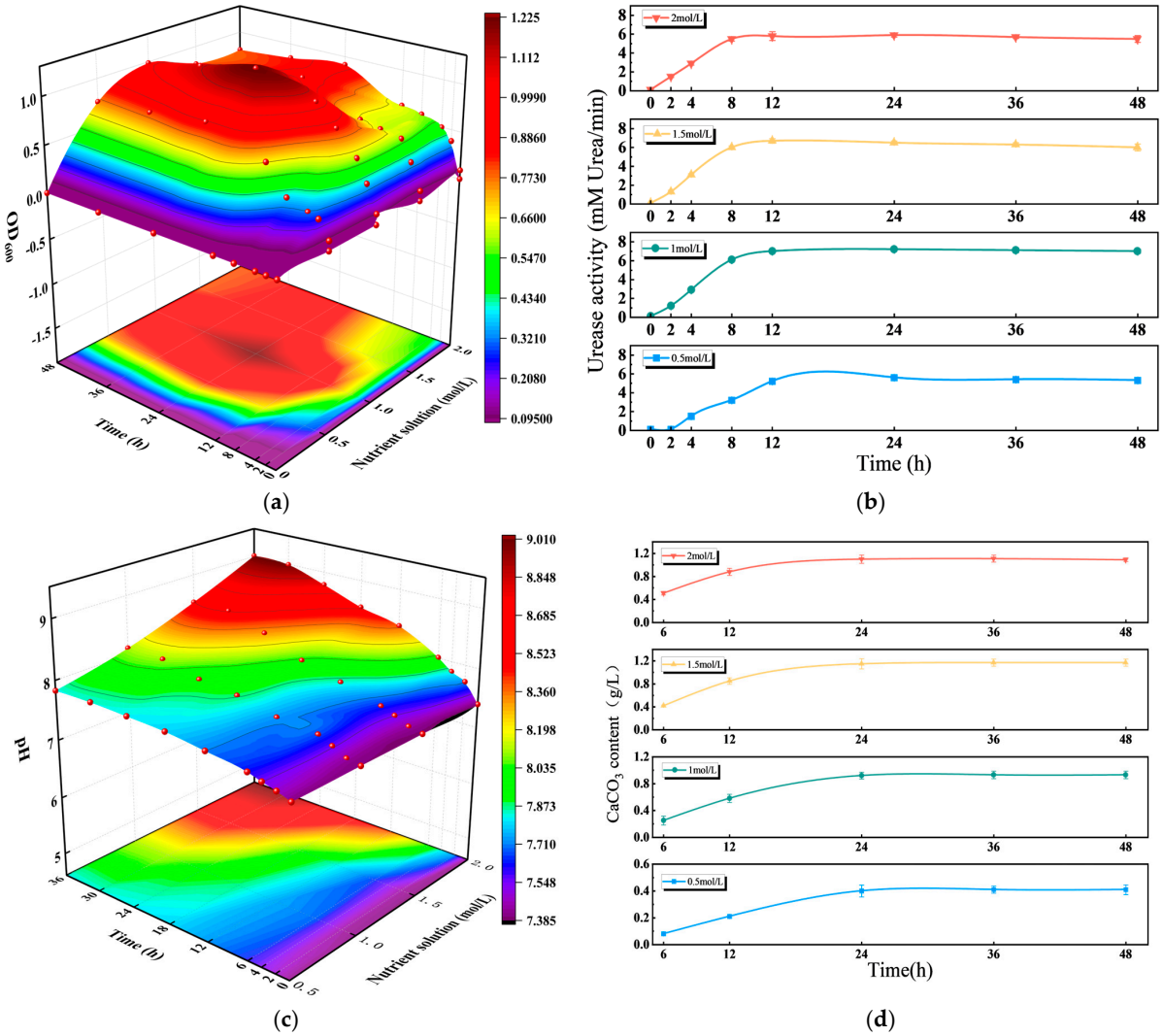


Figure 4. Effect of nutrient solution concentration on bacterial activity: (**a**) The change of OD_{600} with time under different nutrient solution concentrations; (**b**) The changes in urease activity with time under different nutrient solution concentrations; (**c**) the change in pH with time under different nutrient solution concentrations; (**d**) the changes of $CaCO_3$ with time under different nutrient solution concentrations.

3.3. Detection of Residual Amount, Stabilization Efficiency of Bioavailable Heavy Metals and Chemical Form Distribution of Heavy Metals

According to Figure 6a,c,e, the single MICP treatment achieved superior remediation efficiency for Cu, Cd, and Pb compared to the single EK treatment. The incorporation of corn stover biochar, as established in Section 2, further enhances this process by promoting bacterial urease activity and adsorbing heavy metal ions via its porous structure. Consequently, the combined Biochar–MICP–EK treatments (D1–D3) resulted in significantly lower residual heavy metal concentrations and higher stabilization efficiency of bioavailable heavy metals than any single treatment alone. Notably, the D1 formulation yielded the lowest heavy metal content and the highest stabilization efficiency of bioavailable heavy metals among all groups (Tables 5 and 6).

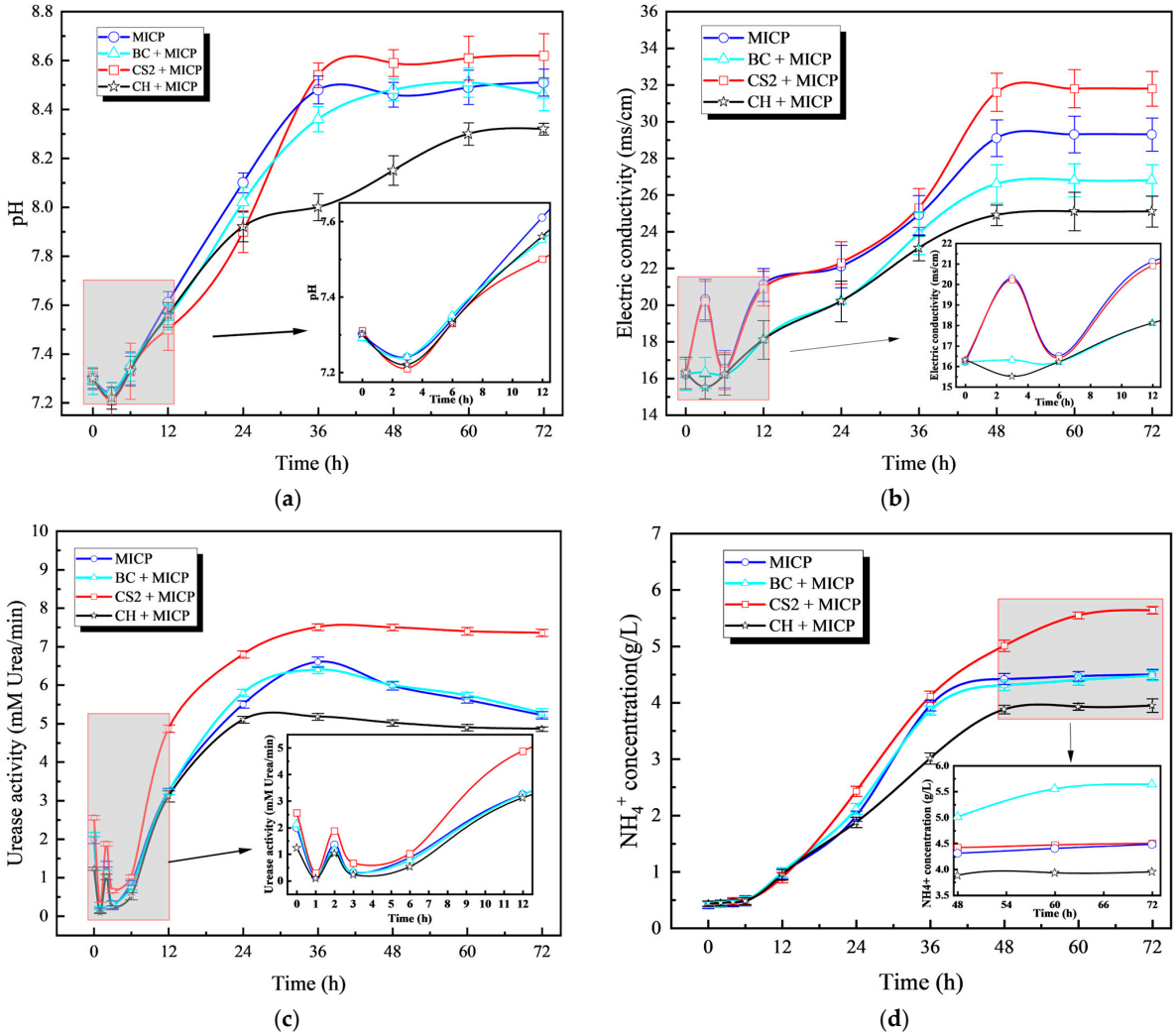


Figure 5. Effect of biochar on MICP process: (**a**) Curve of pH value with time; (**b**) Curve of conductivity with time; (**c**) Curve of urease activity with time; (**d**) Curve of NH_4^+ concentration changing with time.

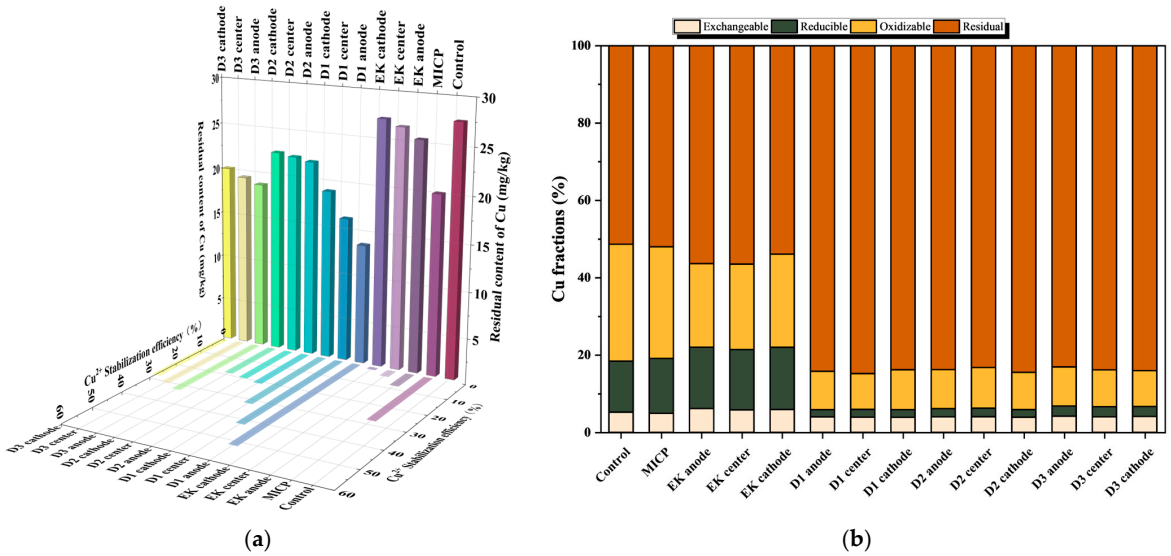
The sequential extraction results for Cu (Figure 6b) demonstrate that the combined treatments (D1–D3) effectively reduced the acid-extractable, reducible, and oxidizable fractions across the anode, middle, and cathode regions compared to individual MICP or EK treatments. This reduction was accompanied by a significant increase in the stable residual fraction, particularly in the anode region [47].

Table 5. The content and Stabilization efficiency of heavy metals in soil after combined treatment changed.

Test Type	Sampling Detection Location	Residual Content of Cu (mg/kg)	Cu^{2+} Stabilization Efficiency (%)	Residual Content of Cd (mg/kg)	Cd^{2+} Stabilization Efficiency (%)	Residual Content of Pb (mg/kg)	Pb^{2+} Stabilization Efficiency (%)
Control	/	27.3		25		65.53	
MICP	/	19.68	27.91	19.02	23.92	56.26	14.15
EK	Anode	25.1	8.06	17.34	30.64	54.82	16.34
	Center	26.23	3.92	20.21	19.16	59.13	9.77
	Cathode	26.9	1.47	22.03	11.88	61.67	5.89
D1	Anode	13.13	51.90	6.65	73.40	41.77	36.26
	Center	15.78	42.20	6.72	73.12	42.10	35.75
	Cathode	18.55	32.05	7.11	71.56	44.66	31.85
D2	Anode	21.54	21.10	15.45	38.20	53.49	18.37
	Center	21.88	19.85	15.90	36.40	53.26	18.72
	Cathode	22.16	18.83	16.22	35.12	56.74	13.41
D3	Anode	18.37	32.71	13.15	47.40	51.74	21.04
	Center	18.96	30.55	13.96	44.16	56.80	13.32
	Cathode	19.77	27.58	15.22	39.12	56.98	13.05

For Cd (Figure 6d) the combined method drastically reduced the acid-extractable fraction in the anode region while substantially increasing the residual fraction. In the middle and cathode regions, the acid-extractable fraction also decreased, and the residual fraction increased, with minimal change in the reducible fraction. The oxidizable fraction first increased and then decreased across the D1–D3 treatments. The D3 group exhibited the lowest residual fraction.

The speciation of Pb (Figure 6f) revealed that the combined method facilitated the transformation of acid-extractable and oxidizable fractions in the anode region into the more stable residual fraction, with similar stabilization trends observed in the middle and cathode regions.



(**a**) (**b**)

Figure 6. *Cont.*

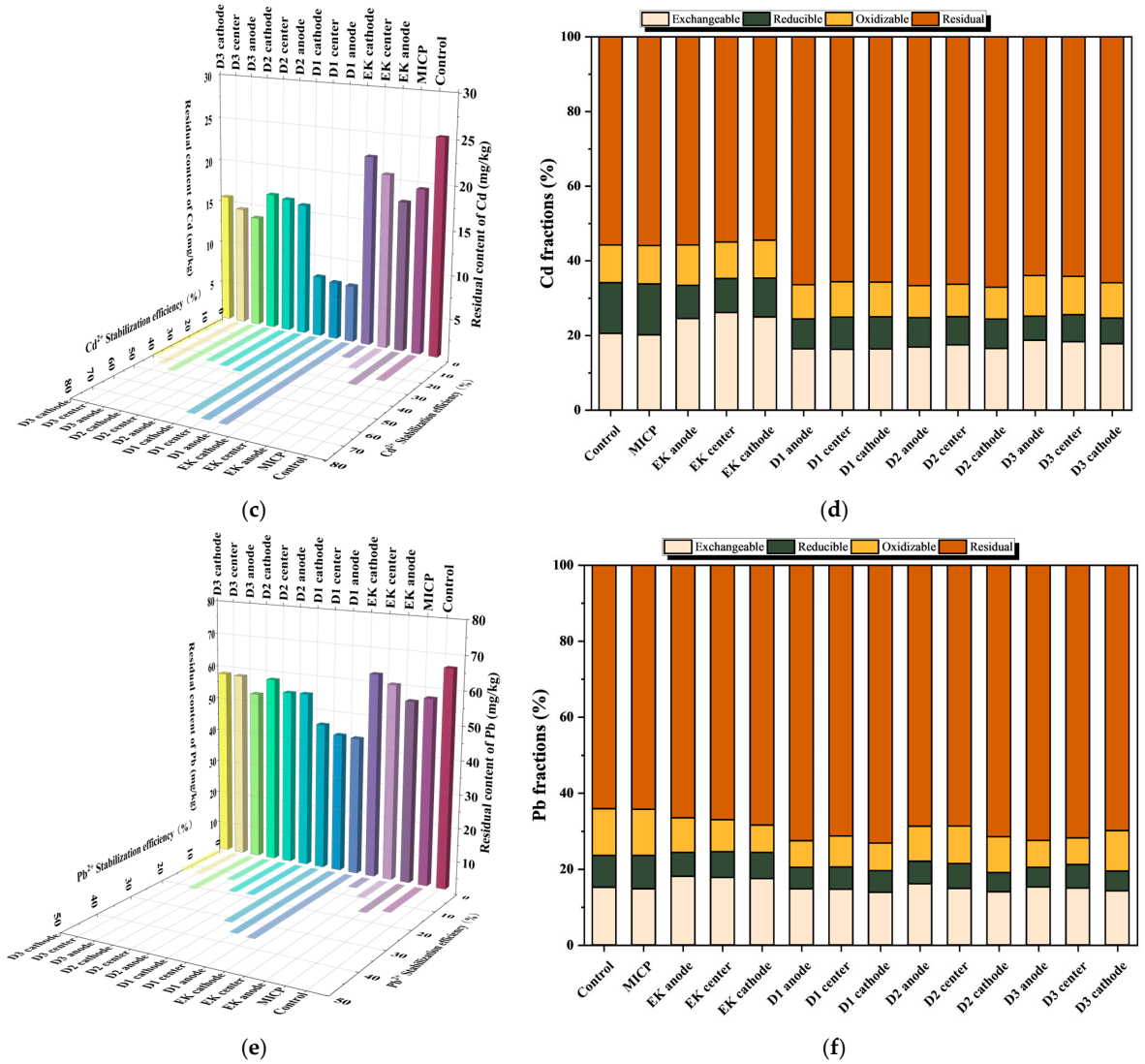


Figure 6. Residual (Heavy metal residue) amount, stabilization efficiency of bioavailable heavy metals, and chemical speciation distribution of Cu, Cd, and Pb after combined remediation: (**a**) Cu residual amount and stabilization efficiency of bioavailable heavy metals; (**b**) Cu chemical speciation; (**c**) Cd residual amount and stabilization efficiency of bioavailable heavy metals; (**d**) Cd chemical speciation; (**e**) Pb residual amount and stabilization efficiency of bioavailable heavy metals; (**f**) Pb chemical speciation.

3.4. Current and Energy Consumption Analysis

Figure 7a compares the current variation across different treatment groups. The initial current was highest in the D3 group, followed by D2 and D1, with D2 and D3 both exceeding the traditional electroosmotic group (EK). As the experiment progressed, all currents decreased gradually. The D1 group consistently maintained the lowest current, ultimately reaching values 12.17%, 63.60%, and 66.80% below those of the EK, D2, and D3 groups, respectively.

The total energy consumption of the D2 and D3 test groups was similar and larger (Figure 7b), and the total energy consumption of the D1 test group was the smallest. The total energy consumption of the D1 test group was 12.16% lower than that of the EK test group, 60.25% lower than that of the D2 test group, and 63.78% lower than that of the D3 test group. In addition, under the four groups of test conditions, the total energy consumption of each test group showed an upward trend. Therefore, from the perspective of energy saving, the D1 test group is better.

Table 6. BCR sequential extraction results of heavy metals (mean ± SD, n = 3, unit: %).

Test Type	Sampling Detection Location	Heavy Metal											
		Cu				Cd				Pb			
		Exchangeable	Reducible	Oxidizable	Residual	Exchangeable	Reducible	Oxidizable	Residual	Exchangeable	Reducible	Oxidizable	Residual
Control	/	5.21 ± 0.6	13.2 ± 1.1	30.25 ± 2.0	51.34 ± 2.5	20.5 ± 1.2	13.6 ± 0.8	10.1 ± 0.5	55.8 ± 2.0	15.2 ± 1.1	8.4 ± 0.9	12.3 ± 1.0	64.1 ± 2.1
MICP	/	4.91 ± 0.7	14.2 ± 1.0	28.9 ± 1.8	51.99 ± 2.0	20.11 ± 1.1	13.66 ± 0.9	10.3 ± 0.6	55.93 ± 1.8	14.81 ± 1.2	8.81 ± 1.1	12.11 ± 0.8	64.27 ± 1.5
EK	Anode	6.13 ± 0.9	15.9 ± 1.5	21.6 ± 1.2	56.37 ± 1.8	24.5 ± 1.5	8.9 ± 0.8	10.8 ± 0.5	55.8 ± 2.1	18.1 ± 0.9	6.3 ± 1.0	9.1 ± 0.6	66.5 ± 1.1
	Center	5.8 ± 0.6	15.6 ± 1.3	22.1 ± 1.4	56.5 ± 2.1	26.1 ± 1.0	9.1 ± 0.5	9.8 ± 0.7	55 ± 1.7	17.8 ± 1.0	6.8 ± 0.8	8.4 ± 0.5	67 ± 0.9
	Cathode	5.9 ± 0.6	16.1 ± 1.2	24.1 ± 1.1	53.9 ± 2.0	24.9 ± 0.8	10.4 ± 0.9	10.2 ± 0.5	54.5 ± 1.3	17.5 ± 0.8	6.9 ± 0.7	7.2 ± 0.4	68.4 ± 1.4
D1	Anode	3.99 ± 0.4	1.88 ± 0.2	9.93 ± 0.8	84.2 ± 2.1	16.35 ± 0.9	8.02 ± 1.0	9.18 ± 0.6	66.45 ± 2.1	14.78 ± 0.4	5.69 ± 0.8	6.99 ± 0.5	72.54 ± 2.1
	Center	3.91 ± 0.5	2.02 ± 0.4	9.28 ± 0.7	84.79 ± 1.9	16.21 ± 1.2	8.68 ± 0.8	9.45 ± 0.7	65.66 ± 2.0	14.68 ± 1.2	5.88 ± 0.9	8.16 ± 0.6	71.28 ± 2.0
	Cathode	3.88 ± 0.7	1.98 ± 0.3	10.34 ± 0.9	83.8 ± 1.8	16.31 ± 1.1	8.65 ± 0.7	9.29 ± 1.0	65.75 ± 1.4	13.88 ± 0.7	5.72 ± 0.4	7.25 ± 0.6	73.15 ± 1.8
D2	Anode	4.01 ± 0.3	2.12 ± 0.2	10.09 ± 0.6	83.78 ± 1.5	16.86 ± 0.8	7.89 ± 0.8	8.56 ± 1.1	66.69 ± 1.9	16.12 ± 0.6	5.96 ± 0.7	9.21 ± 1.0	68.71 ± 1.6
	Center	4.04 ± 0.5	2.21 ± 0.3	10.52 ± 0.5	83.23 ± 1.8	17.44 ± 0.9	7.56 ± 0.3	8.66 ± 0.9	66.34 ± 1.8	14.89 ± 0.5	6.58 ± 0.6	9.86 ± 0.8	68.67 ± 1.4
	Cathode	3.89 ± 0.4	2.01 ± 0.1	9.61 ± 1.0	84.49 ± 1.9	16.46 ± 1.0	7.89 ± 0.5	8.52 ± 0.8	67.13 ± 1.7	14.03 ± 0.5	5.05 ± 0.3	9.45 ± 1.0	71.47 ± 1.3
D3	Anode	4.16 ± 0.7	2.66 ± 0.1	10.1 ± 0.4	83.08 ± 2.0	18.66 ± 2.1	6.46 ± 0.4	10.88 ± 0.9	64 ± 1.3	15.26 ± 0.5	5.21 ± 0.5	7.05 ± 0.7	72.48 ± 1.0
	Center	4.02 ± 0.4	2.61 ± 0.2	9.55 ± 0.6	83.82 ± 1.4	18.28 ± 1.8	7.26 ± 0.6	10.22 ± 1.1	64.24 ± 2.0	14.98 ± 0.7	6.22 ± 0.8	6.98 ± 0.8	71.82 ± 1.6
	Cathode	4.09 ± 0.8	2.59 ± 0.4	9.26 ± 0.5	84.06 ± 1.5	17.75 ± 0.9	6.86 ± 0.5	9.46 ± 0.6	65.93 ± 2.1	14.23 ± 1.1	5.24 ± 0.6	10.66 ± 0.9	69.87 ± 1.8

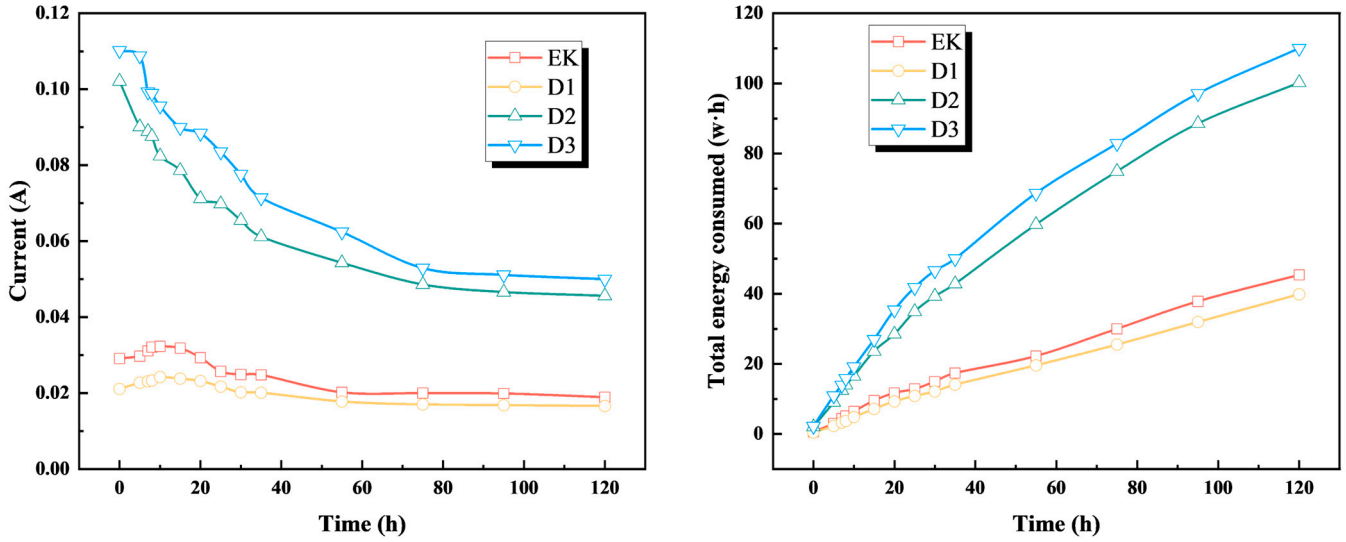


Figure 7. Current and energy consumption diagram after treatment of contaminated soil: (**a**) The current diagram after processing; (**b**) Total energy consumption diagram after treatment.

3.5. Toxicity Characteristic Leaching Procedure Test Results

As shown in Figure 8, the leachate concentrations of Cu, Cd, and Pb from the combined treatments (D1–D3) were significantly lower than those from the individual MICP or EK treatments and were all below the regulatory limit specified in the "Hazardous Waste Identification Standard-Leaching Toxicity Identification" (GB5085.3-2007) [48]. Notably, the D1 group achieved the lowest leachate concentration for Cu and Pb in the anode region, while Cd was undetectable in the anode leachate of both the D1 and D3 groups. The method detection limit of TCLP was Cu: 100 mg/L, Cd: 1 mg/L, and Pb: 5 mg/L. The "not detected" indicated that the Cd concentration was less than the detection limit of the method and could not be evaluated.

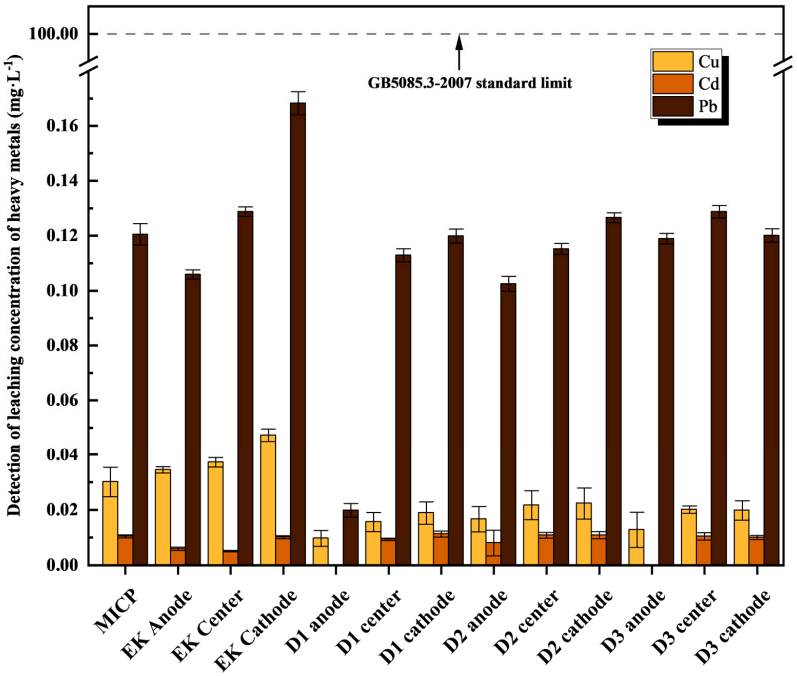


Figure 8. Detection of leaching concentration of heavy metals after treatment of contaminated soil by combined method.

3.6. X-Ray Diffraction and Scanning Electron Microscopy Results

The XRD patterns of the mineralization products with different biochar additions are shown in Figure 9a. The type of biochar significantly influenced the crystal phase of the precipitates. The addition of coconut shell biochar led to the disappearance of characteristic calcite peaks and the emergence of new peaks at 2θ = 27.1°, 32°, and 42.2°, which were identified as vaterite. In contrast, both corn stover and bamboo biochar promoted the crystallization of calcite, yielding sharper diffraction peaks. The most intense calcite peak at 2θ = 29.3° was observed with corn stover biochar.

Figure 9b presents the XRD patterns of soils subjected to different remediation methods (undisturbed soil, MICP-only, EK-only, and the combined D-series treatments). The formation of heavy metal carbonates (e.g., $PbCO_3$, $CdCO_3$) and changes in hydroxide phases (e.g., $Cu(OH)_2$, $Pb(OH)_2$) were detected in the D-series groups. Although the treatment sequence (D1–D3) did not alter the final mineral phases, it significantly affected their crystallinity, as reflected in the peak intensities. The D1 group exhibited the sharpest diffraction peaks for stable phases and the weakest signals for original heavy metal pollutants in the soil.

SEM analysis revealed distinct morphological changes in the soil induced by different remediation methods. The original contaminated soil exhibited massive crystals with clear interstitial gaps (Figure 10a). Soils treated with EK or MICP alone showed a plate-like agglomerated structure (Figure 10b,c). In contrast, the combined remediation methods (Figure 10d–f) promoted more complete microbial-induced mineralization, forming a dense, compact microstructure with well-developed macro-aggregates.

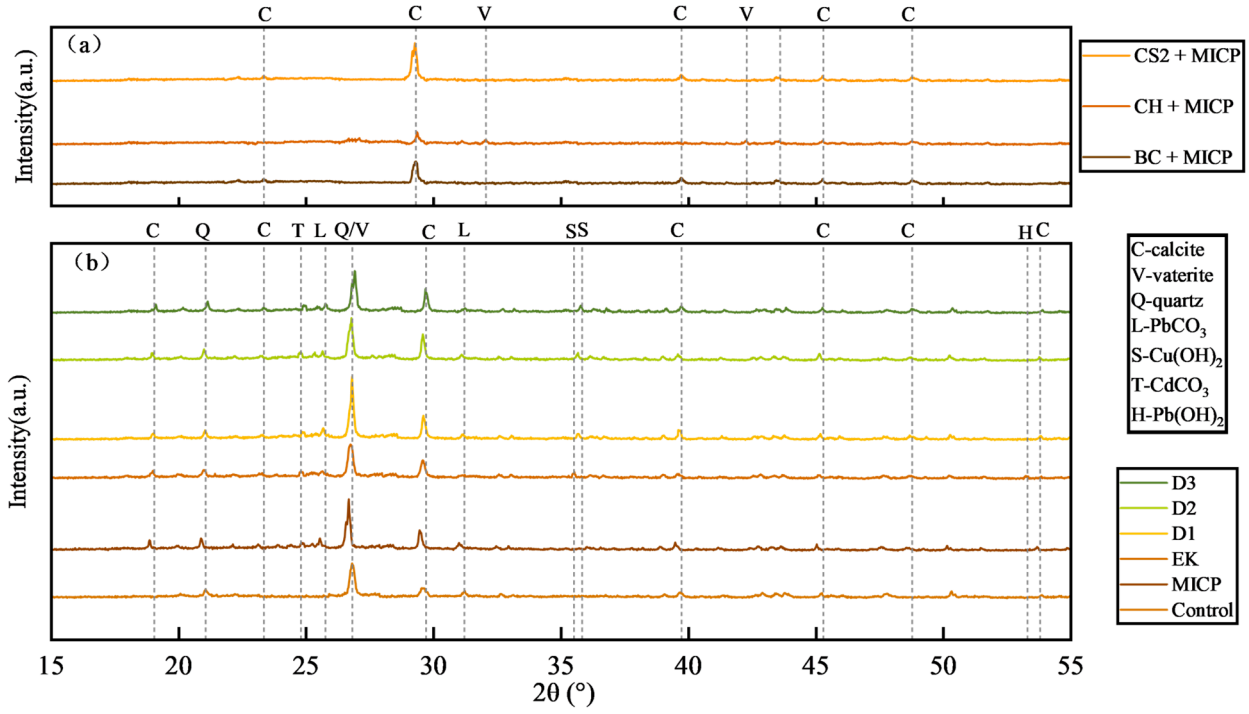
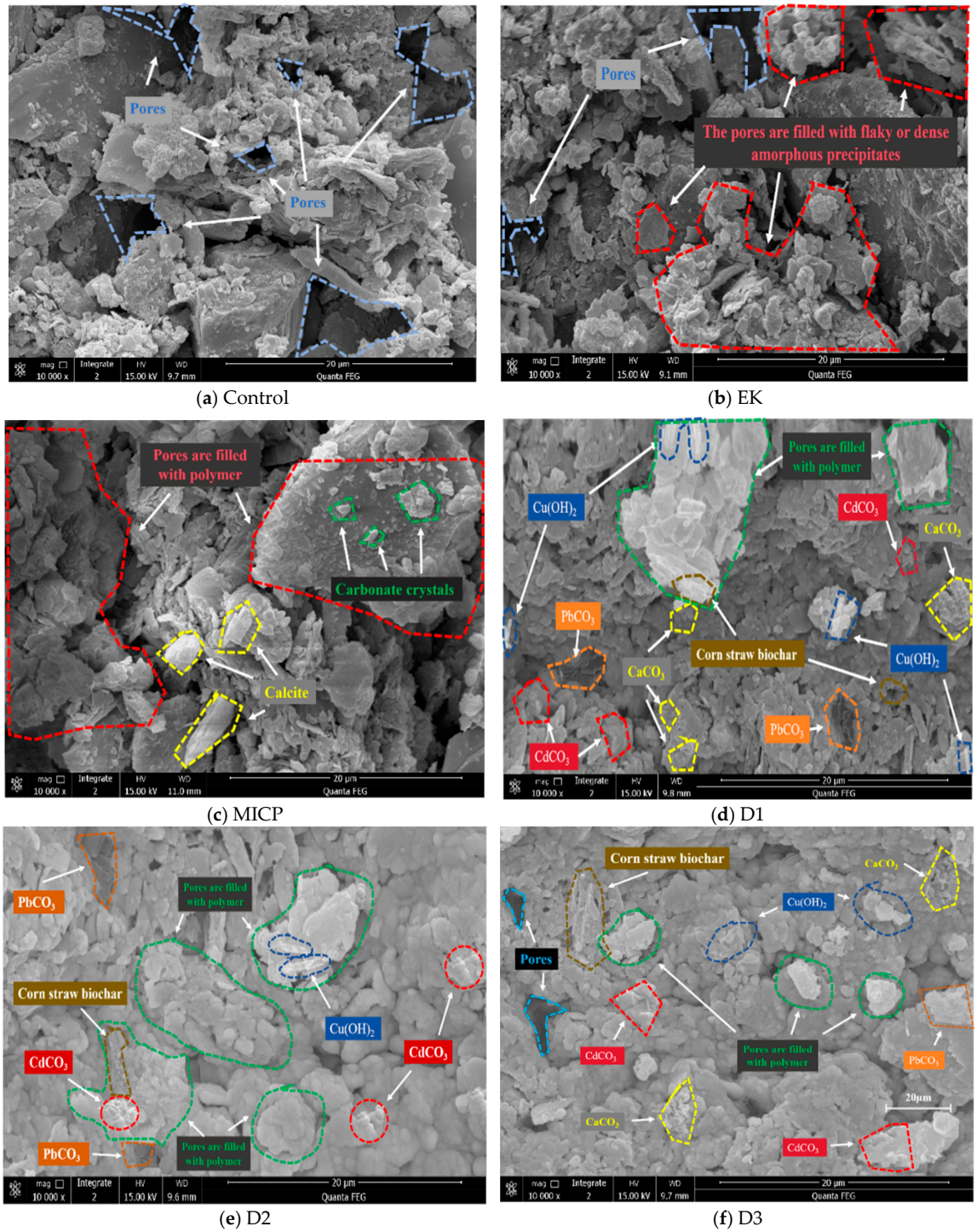


Figure 9. Changes in mineral composition after remediation of contaminated soil by combined method: (**a**) XRD results of soil after adding three biochars; (**b**) Soil XRD results after the combined method test.

3.7. Pearson Correlation Analysis Results

Figure 11 presents a correlation heatmap illustrating the relationships among heavy metal content, stabilization efficiency, pH, electrical conductivity (EC), urease activity, and NH_4^+ concentration in soil treated with the combined method. A strong positive correlation

was observed between OD_{600} (microbial density) and urease activity. Both parameters were positively correlated with the stabilization efficiency of bioavailable fractions of the three heavy metals (Cu, Cd, Pb). Accordingly, the stabilization efficiency of bioavailable heavy metals exhibited a significant positive correlation with pH. In contrast, EC showed only a weak correlation with NH_4^+ concentration, heavy metal residue, and stabilization efficiency of bioavailable heavy metals.



(**a**) Control (**b**) EK

(**c**) MICP (**d**) D1

(**e**) D2 (**f**) D3

Figure 10. SEM results of soil samples.

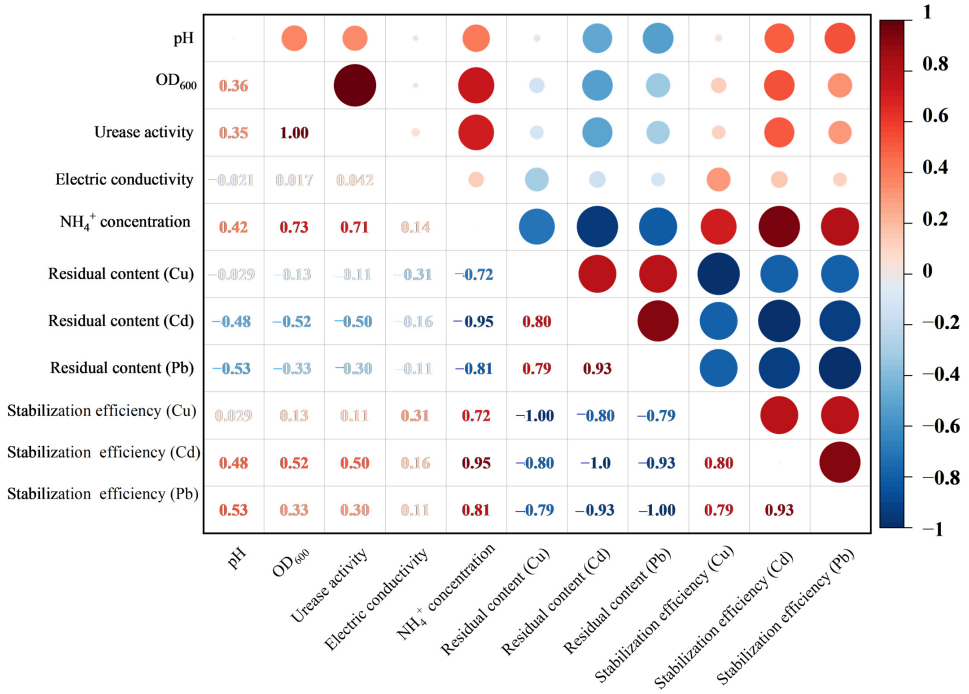


Figure 11. Pearson correlation heatmap between heavy metal content, stabilization efficiency of bioavailable heavy metals, pH, and electrical conductivity of contaminated soil after combined remediation.

4. Discussion

4.1. Conclusion of Effect of Nutrient Solution Concentration on Bacterial Activity

The optimal nutrient concentration of 1 mol/L urea–$CaCl_2$ identified in this study aligns with the findings of Raja et al. [44], who emphasized that excessive nutrient concentrations (e.g., 2 mol/L) can cause osmotic stress on microbial cells, thereby inhibiting metabolic activity. The stable pH range (7.8–8.2) maintained by the 1 mol/L group is critical for MICP, as reported by Mahdi et al. [45], who noted that urease activity is maximized at pH 7.5–8.5. Although higher concentrations (1.5–2 mol/L) yielded slightly more $CaCO_3$, the compromised microbial activity and unstable pH make them unsuitable for long-term remediation. Thus, 1 mol/L urea–$CaCl_2$ balances "environmental suitability-microbial activity-product efficiency-cost-effectiveness," providing a practical benchmark for MICP applications.

4.2. Conclusion of the Effect of Biochar on the MICP Process

The stimulatory effect of corn stover biochar on urease activity can be attributed to its high specific surface area (580 m^2/g) and abundant oxygen-containing functional groups (-COOH, -OH), which provide adsorption sites for heavy metals and nutrients for microbes involved in MICP [24,25]. In contrast, coconut shell biochar's inhibitory effect may stem from its high ash content and alkaline nature (pH > 10), which disrupt the optimal pH range for microbial growth [49]. Bamboo biochar's neutral impact is likely due to its moderate porosity and low heavy metal adsorption capacity, resulting in no significant interference with MICP. These results highlight the importance of biochar selection. Corn stover biochar, derived from agricultural waste, is not only cost-effective but also enhances MICP efficiency, thus making it a promising amendment for combined remediation.

4.3. Stabilization Efficiency and Chemical Speciation of Heavy Metals

The superior performance of the D1 group (EK pretreatment followed by MICP) can be explained by the synergistic effects of EK, biochar, and MICP. EK first mobilizes heavy metals from stable fractions, as reported by Acar et al. [29], creating a concentrated target for subsequent MICP. Biochar then adsorbs the mobilized metals, reducing their toxicity to microbes and providing nucleation sites for carbonate precipitation [47]. MICP finally converts the adsorbed metals into stable carbonate minerals (e.g., $CdCO_3$, $PbCO_3$), as confirmed by XRD analysis. The significant increase in the residual fraction (Figure 6b,d,f) indicates that heavy metals are transformed into inert forms, reducing their bioavailability and leachability [50]. The lower residual fraction in the D3 group (MICP followed by EK) is due to EK-induced remobilization of newly precipitated carbonates in the acidic anode region, emphasizing the importance of treatment sequence.

4.4. Current and Energy Consumption

The lower current and energy consumption of the D1 group can be attributed to EK pretreatment, which reduces soil electrical resistance by removing soluble salts and improving porosity [34]. In contrast, the D2 and D3 groups experience higher resistance due to simultaneous EK and MICP/biochar addition—biochar's high conductivity initially increases current, but subsequent carbonate precipitation clogs pores, raising resistance and energy consumption [29]. The D1 group's energy consumption (27.49% lower than EK group) is comparable to the optimized EK systems reported by Cameselle et al. [21], demonstrating the energy-saving potential of the combined technology.

4.5. Conclusion of Toxicity Characteristic Leaching Procedure

The low leachate concentrations in the D1 group confirm the long-term stability of the stabilized heavy metals. EK's migration of cationic metals (Cu^{2+}, Cd^{2+}, Pb^{2+}) toward the cathode reduces their concentration in the anode region, explaining the lowest leachate levels there [48]. The undetectable Cd in the D1 and D3 anode leachates indicates complete stabilization, as $CdCO_3$ has extremely low solubility (Ksp = 1.0×10^{-12}) [17]. These results meet the regulatory requirements of GB5085.3-2007, validating the environmental safety of the combined technology.

4.6. Microstructural and Mineralogical Changes

The formation of stable calcite in the D1 group (XRD Figure 9a) enhances soil aggregation and reduces compaction (SEM Figure 10d), addressing a major limitation of single EK or MICP treatments [42]. Calcite acts as a cementing agent, improving soil shear strength and permeability, making the remediated soil suitable for agricultural or engineering use [43]. The vaterite formation in the coconut shell biochar group is undesirable, as vaterite is metastable and can transform into calcite over time, potentially releasing heavy metals [46]. Thus, corn stover biochar is preferred for promoting stable calcite formation.

4.7. Pearson Correlation Analysis Conclusion

The strong positive correlation between OD_{600} and urease activity (Figure 11) confirms that microbial growth is closely linked to metabolic function. The positive correlation between urease activity and stabilization efficiency indicates that MICP is the key driver of heavy metal stabilization [44]. The positive correlation between pH and stabilization efficiency is due to the role of alkaline conditions in promoting carbonate precipitation [45]. The weak correlation between EC and other parameters suggests that EC is influenced by multiple factors (e.g., soluble salts, biochar, carbonate precipitation) and is not a reliable indicator of remediation efficacy alone.

5. Future Perspectives

Future research can further optimize the combination mode and parameters of the three technologies. For example, exploring the optimal time interval between EK pretreatment and MICP can avoid the adverse effect of the electric field on microbial activity. Adjusting the dosage and addition time of biochar can maximize its synergistic effect with EK and MICP. In addition, the integration of intelligent control systems into the combined system can monitor the soil pH, electrical conductivity, and heavy metal concentration in real time, and adjust the EK voltage, MICP nutrient concentration, and other parameters according to the monitoring results, realizing the intelligent and efficient operation of the remediation process.

6. Conclusions

This study investigated the remediation of heavy metal-contaminated soil using individual (EK, MICP) and combined (Biochar–MICP–EK) approaches. The immobilization effectiveness was evaluated through measurements of residual heavy metal content, chemical speciation, and leaching toxicity. The main findings are as follows:

1. An optimal nutrient concentration of 1 mol/L urea–$CaCl_2$ was identified, which balanced high bacterial cell density (OD_{600} = 1.0), urease activity (12 U/g), and stable pH (7.8–8.2), providing a cost-effective benchmark for application, while higher concentrations inhibited microbial activity.
2. Corn stover biochar significantly enhanced urease activity, whereas coconut shell biochar exhibited an inhibitory effect, and bamboo biochar showed a neutral impact.
3. The combined Biochar–MICP–EK remediation was significantly more effective than any single method. The D1 treatment protocol (EK pretreatment followed by MICP) achieved the most effective immobilization of Cu, Cd, and Pb, markedly increasing the stable residual fraction.
4. Microstructural and mineralogical analyses revealed that the combined method improved soil aggregation and promoted the formation of stable calcite. The synergistic mechanism involves electric field-driven ion migration, biochar adsorption, and MICP-induced carbonate precipitation. Among all tested groups, D1 demonstrated superior overall performance: it yielded the highest heavy metal immobilization efficiency, achieved the most significant transformation of heavy metals to stable residues, and had the lowest energy consumption.

Author Contributions: Conceptualization, Methodology, Supervision, Writing—review and editing, Proofreading the article, P.L.; Validation, Writing—original and Investigation, R.W.; Investigation, Data analysis, W.W.; Methodology, editing, R.W. All authors have read and agreed to the published version of the manuscript.

Funding: This research received no external funding.

Institutional Review Board Statement: Not applicable.

Informed Consent Statement: Not applicable.

Data Availability Statement: The original contributions presented in this study are included in the article. Further inquiries can be directed to the corresponding author.

Acknowledgments: The author would like to express his gratitude to all those who have given support and assistance during the research and writing of this paper.

Conflicts of Interest: The remaining authors declare that the research was conducted in the absence of any commercial or financial relationships that could be construed as a potential conflict of interest.

Abbreviations

The following abbreviations are used in this manuscript:

EK	Electrokinetic Remediation
EC	Electrical Conductivity
UA	Urease Activity
MICP	Microbial-Induced Calcium Carbonate Precipitation
TCLP	Toxicity Characteristic Leaching Procedure
PRB	Permeable Reactive Barrier
FAAS	Flame Atomic Absorption Spectrophotometry
BCR	European Community Bureau of Reference
XRD	X-ray Diffraction
SEM	Scanning Electron Microscopy
OD_{600}	Optical Density at 600 nm
D1	Reaction sequence: EK →Biochar +MICP
D2	Reaction sequence: EK + Biochar + MICP
D3	Reaction sequence: Biochar +MICP→EK

References

1. Namadi, A.H.; Motlagh, A.H.; Hassanlourad, M.; Hosseinzadeh, M. Impact of Heavy Metal and Carbonate on Geotechnical Properties of Sand-Bentonite Mixtures. *Indian Geotech. J.* **2023**, *53*, 1494–1504. [CrossRef]
2. Montaño-López, F.; Biswas, A. Are heavy metals in urban garden soils linked to vulnerable populations? *A case study from Guelph, Canada. Sci. Rep.* **2021**, *11*, 11286. [CrossRef]
3. Oloruntoba, A.; Omoniyi, A.O.; Shittu, Z.A.; Ajala, R.O.; Kolawole, S.A. Heavy Metal Contamination in Soils, Water, and Food in Nigeria from 2000–2019: A Systematic Review on Methods, Pollution Level and Policy Implications. *Water Air Soil Pollut.* **2024**, *235*, 586. [CrossRef]
4. Liu, N.; Zhao, J.; Du, J.; Hou, C.; Zhou, X.; Chen, J.; Zhang, Y. Non-phytoremediation and phytoremediation technologies of integrated remediation for water and soil heavy metal pollution: A comprehensive review. *Sci. Total. Environ.* **2024**, *948*, 174237. [CrossRef]
5. Xie, S.; Wu, F.; Ning, Z.; Chen, M.; Liu, C.; Huang, Q.; Meng, F.; Liu, Y.; Zhou, J.; Xia, Y. Two-step calculation method to enable the ecological and human health risk assessment of remediated soil treated through thermal curing. *Soil Ecol. Lett.* **2021**, *3*, 266–278. [CrossRef]
6. Zang, X.; Zhang, Y.; Yue, H. Study on the effect of using multi-round citric acid bottom vacuum leaching to remediate Cu, Zn-contaminated soil. *Front. Environ. Sci.* **2025**, *13*, 1646182. [CrossRef]
7. Wang, L.; Rinklebe, J.; Tack, F.M.G.; Hou, D. A review of green remediation strategies for heavy metal contaminated soil. *Soil Use Manag.* **2021**, *37*, 936–963. [CrossRef]
8. Virkutyte, J.; Sillanpää, M.; Latostenmaa, P. Electrokinetic soil remediation—Critical overview. *Sci. Total. Environ.* **2002**, *289*, 97–121. [CrossRef] [PubMed]
9. Yeung, A.T.; Gu, Y.-Y. A review on techniques to enhance electrochemical remediation of contaminated soils. *J. Hazard. Mater.* **2011**, *195*, 11–29. [CrossRef]
10. Reddy, K.R.; Cameselle, C. *Electrochemical Remediation Technologies for Polluted Soils, Sediments and Groundwater*; John Wiley & Sons, Inc.: Hoboken, NJ, USA, 2009.
11. Song, Y.; Cang, L.; Fang, G.; Ata-Ul-Karim, S.T.; Xu, H.; Zhou, D. Electrokinetic delivery of anodic in situ generated active chlorine to remediate diesel-contaminated sand. *Chem. Eng. J.* **2018**, *337*, 499–505. [CrossRef]
12. Gill, R.T.; Harbottle, M.J.; Smith, J.W.N.; Thornton, S.F. Electrokinetic-enhanced bioremediation of organic contaminants: A review of processes and environmental applications. *Chemosphere* **2014**, *107*, 31–42. [CrossRef] [PubMed]
13. Wang, Y.; Han, Z.; Li, A.; Cui, C. Enhanced electrokinetic remediation of heavy metals contaminated soil by biodegradable complexing agents. *Environ. Pollut.* **2021**, *283*, 117111. [CrossRef]
14. Fardin, A.B.; Jamshidi-Zanjani, A. A critical review on soil remediation using electrokinetic-enhanced permeable reactive barriers: Challenges and enhancements. *Chem. Eng. J. Adv.* **2025**, *23*, 100774. [CrossRef]
15. Moghadam, M.J.; Moayedi, H.; Sadeghi, M.M.; Hajiannia, A. A review of combinations of electrokinetic applications. *Environ. Geochem. Health* **2016**, *38*, 1217–1227. [CrossRef]

16. Warren, L.A.; Maurice, P.A.; Parmar, N.; Ferris, F.G. Microbially Mediated Calcium Carbonate Precipitation: Implications for Interpreting Calcite Precipitation and for Solid-Phase Capture of Inorganic Contaminants. *Geomicrobiol. J.* **2001**, *18*, 93–115. [CrossRef]
17. Li, M.; Cheng, X.; Guo, H. Heavy metal removal by biomineralization of urease producing bacteria isolated from soil. *Int. Biodeterior. Biodegrad.* **2013**, *76*, 81–85. [CrossRef]
18. Mugwar, A.J.; Harbottle, M.J. Toxicity effects on metal sequestration by microbially-induced carbonate precipitation. *J. Hazard. Mater.* **2016**, *314*, 237–248. [CrossRef]
19. Juillot, F.; Ildefonse, P.; Morin, G.; Calas, G.; Kersabiec, A.; Benedetti, M. Remobilization of arsenic from buried wastes at an industrial site: Mineralogical and geochemical control. *Appl. Geochem.* **1999**, *14*, 1031–1048. [CrossRef]
20. Kang, C.-H.; Han, S.-H.; Shin, Y.; Oh, S.J.; So, J.-S. Bioremediation of Cd by Microbially Induced Calcite Precipitation. *Appl. Biochem. Biotechnol.* **2014**, *172*, 2907–2915. [CrossRef]
21. Cameselle, C.; Reddy, K.R. Development and enhancement of electro-osmotic flow for the removal of contaminants from soils. *Electrochim. Acta* **2012**, *86*, 10–22. [CrossRef]
22. Peng, D.; Chen, X.; Zhang, S.; Zeng, G.; Yan, C.; Luo, H.; Liu, H.; Xu, H. Biochar enhances Cd mineralization through microbially induced carbonate precipitation as a soil remediation strategy for rice paddies. *Chemosphere* **2024**, *366*, 143441. [CrossRef] [PubMed]
23. Xu, M.; Ma, J.; Zhang, X.-H.; Yang, G.; Long, L.-L.; Chen, C.; Song, C.; Wu, J.; Gao, P.; Guan, D.-X. Biochar-bacteria partnership based on microbially induced calcite precipitation improves Cd immobilization and soil function. *Biochar* **2023**, *5*, 20. [CrossRef]
24. Zhang, X.; Wang, H.; He, L.; Lu, K.; Sarmah, A.; Li, J.; Bolan, N.S.; Pei, J.; Huang, H. Using biochar for remediation of soils contaminated with heavy metals and organic pollutants. *Environ. Sci. Pollut. Res.* **2013**, *20*, 8472–8483. [CrossRef]
25. Bashir, S.; Rehman, M.; Yousaf, M.; Salam, A.; Gulshan, A.B.; Iqbal, J.; Aziz, I.; Azeem, M.; Rukh, S.; Asghar, R.M.A. Comparative efficiency of wheat straw and sugarcane bagasse biochar reduces the cadmium bioavailability to spinach and enhances the microbial activity in contaminated soil. *Int. J. Phytoremediat.* **2019**, *21*, 1098–1103. [CrossRef]
26. Tan, X.; Liu, Y.; Gu, Y.; Zeng, G.; Hu, X.; Wang, X.; Hu, X.; Guo, Y.; Zeng, X.; Sun, Z. Biochar amendment to lead-contaminated soil: Effects on fluorescein diacetate hydrolytic activity and phytotoxicity to rice. *Environ. Toxicol. Chem.* **2015**, *34*, 1962–1968. [CrossRef]
27. Li, L.; Jia, Z.; Ma, H.; Bao, W.; Li, X.; Tan, H.; Xu, F.; Xu, H.; Li, Y. The effect of two different biochars on remediation of Cd-contaminated soil and Cd uptake by Lolium perenne. *Environ. Geochem. Health* **2019**, *41*, 2067–2080. [CrossRef]
28. Mulligan, C.N.; Yong, R.N.; Gibbs, B.F. Remediation technologies for metal-contaminated soils and groundwater: An evaluation. *Eng. Geol.* **2001**, *60*, 193–207. [CrossRef]
29. Acar, Y.B.; Alshawabkeh, A.N. Principles of electrokinetic remediation. *Environ. Sci. Technol.* **1993**, *27*, 2638–2647. [CrossRef]
30. Gadd, G.M. Metals, minerals and microbes: Geomicrobiology and bioremediation. *Microbiology* **2010**, *156 Pt 3*, 609–643. [CrossRef]
31. Bolan, N.; Kunhikrishnan, A.; Thangarajan, R.; Kumpiene, J.; Park, J.; Makino, T.; Kirkham, M.B.; Scheckel, K. Remediation of heavy metal(loid)s contaminated soils—To mobilize or to immobilize? *J. Hazard. Mater.* **2014**, *266*, 141–166. [CrossRef]
32. *GB/T 50123-2019*; Standard for Geotechnical Testing Methods. China Planning Publishing House: Beijing, China, 2019.
33. *D 2487-17*; ASTM Standard Practice for Classification of Soils for Engineering Purposes (Unified Soil Classification System). ASTM: West Conshehoken, PA, USA, 2017.
34. Jiaqing, Y.; Shukui, Z.; Yi, T.; Yingjiu, L.; Ye, Z.; Weiyan, Z.; Dongchun, L.; Chaofan, X. Research progress on electrokinetic-leaching combined remediation of heavy metal contaminated soil. *Appl. Chem. Ind.* **2022**, *51*, 3634–3640. [CrossRef]
35. *GB 15618-2018*; Soil Environmental Quality Standard-Risk Control Standard for Soil Pollution of Agricultural Land. China Environmental Science Press: Beijing, China, 2018.
36. Lauchnor, E.G.; Topp, D.M.; Parker, A.E.; Gerlach, R. Whole cell kinetics of ureolysis by *Sporosarcina pasteurii*. *J. Appl. Microbiol.* **2015**, *118*, 1321–1332. [CrossRef] [PubMed]
37. Rauret, G.; López-Sánchez, J.F.; Sahuquillo, A.; Rubio, R.; Davidson, C.; Ure, A.; Quevauviller, P. Improvement of the BCR three step sequential extraction procedure prior to the certification of new sediment and soil reference materials. *J. Environ. Monit.* **1999**, *1*, 57–61. [CrossRef]
38. Qian, W. Study on Microbial Curing Modification Mechanism and Anti-Liquefation Property of Silt in the Middle and Lower Reaches of Yellow River. Master's Thesis, North China University of Water Resources and Electric Power, Zhengzhou, China, 2022.
39. *HJ802-2016*; Soil-Determination of Conductivity-Electrode Method. China Environmental Science Press: Beijing, China, 2016.
40. *HJ/T-299-2007*; Solid Waste-Extraction Procedure for Leaching Toxicity Sulphuric Acid & Nitric Acid Method. China Environmental Science Press: Beijing, China, 2007.
41. Schommer, V.A.; Vanin, A.P.; Nazari, M.T.; Ferrari, V.; Dettmer, A.; Colla, L.M.; Piccin, J.S. Biochar-immobilized Bacillus spp. for heavy metals bioremediation: A review on immobilization techniques, bioremediation mechanisms and effects on soil. *Sci. Total. Environ.* **2023**, *881*, 163385. [CrossRef] [PubMed]

42. Liu, B.; Tang, C.-S.; Pan, X.-H.; Cheng, Q.; Shen, Z.-T.; Xu, J.-J.; Zhang, X.-Y. Influence of layer thickness on bioremediation of drought-induced soil desiccation cracks using microbially induced calcite precipitation. *Acta Geotech.* **2023**, *19*, 4399–4414. [CrossRef]
43. Li, Y.; Zhang, M.; Wang, X.; Ai, S.; Meng, X.; Liu, Z.; Yang, F.; Cheng, K. Synergistic enhancement of cadmium immobilization and soil fertility through biochar and artificial humic acid-assisted microbial-induced calcium carbonate precipitation. *J. Hazard. Mater.* **2024**, *476*, 135140. [CrossRef]
44. Murugan, R.; Suraishkumar, G.K.; Mukherjee, A.; Dhami, N.K. Insights into the influence of cell concentration in design and development of microbially induced calcium carbonate precipitation (MICP) process. *PLoS ONE* **2021**, *16*, e0254536. [CrossRef]
45. Maleki-Kakelar, M.; Azarhoosh, M.J.; Senji, S.G.; Aghaeinejad-Meybodi, A. Urease production using corn steep liquor as a low-cost nutrient source by Sporosarcina pasteurii: Biocementation and process optimization via artificial intelligence approaches. *Environ. Sci. Pollut. Res.* **2021**, *29*, 13767–13781. [CrossRef]
46. Kim, Y.; Roh, Y. Microbially Induced Carbonate Precipitation Using Microorganisms Enriched from Calcareous Materials in Marine Environments and Their Metabolites. *Minerals* **2019**, *9*, 722. [CrossRef]
47. Tu, C.; Wei, J.; Guan, F.; Liu, Y.; Sun, Y.; Luo, Y. Biochar and bacteria inoculated biochar enhanced Cd and Cu immobilization and enzymatic activity in a polluted soil. *Environ. Int.* **2020**, *137*, 105576. [CrossRef] [PubMed]
48. *GB5085.3-2007*; Identification Standards for Hazardous Wastes-Identification for Extraction Toxicity. China Standards Press: Beijing, China, 2007.
49. Mi, L. Acid-Base Properties, Alkali and Alkaline Earth Metallic Species leaching and Cu (II) Sorption by Aquatic Plant-Derive Biochar. Master's Thesis, Shanghai University, Nanjing, China, 2014.
50. Wei, T.; Li, X.; Li, H.; Gao, H.; Guo, J.; Li, Y.; Ren, X.; Hua, L.; Jia, H. The potential effectiveness of mixed bacteria-loaded biochar/activated carbon to remediate Cd, Pb co-contaminated soil and improve the performance of pakchoi plants. *J. Hazard. Mater.* **2022**, *435*, 129006. [CrossRef] [PubMed]

Disclaimer/Publisher's Note: The statements, opinions and data contained in all publications are solely those of the individual author(s) and contributor(s) and not of MDPI and/or the editor(s). MDPI and/or the editor(s) disclaim responsibility for any injury to people or property resulting from any ideas, methods, instructions or products referred to in the content.